Undulations in Salt-Free Charged Lamellar Phases Detected by Small Angle Neutron Scattering and Neutron Reflectivity†

Golchi Salamat, Renko de Vries, and Eric W. Kaler*

Center for Molecular and Engineering Thermodynamics, Department of Chemical Engineering, University of Delaware, Newark, Delaware 19716

Sushil Satija and Lipiin Sung

Center for Neutron Research, National Institute of Standards and Technology, Gaithersburg, Maryland 20817

Received May 11, 1999

Neutron reflectivity of lamellar phases containing pentaethylene glycol *n*-dodecyl ether, sodium decylsulfonate, and D_2O is measured at the solid−liquid interface. The scattering length density profiles deduced from fits to the reflectivity data show that undulations of the mixed surfactant bilayers close to the solid−liquid interface decrease as the molar ratio of ionic to nonionic surfactant increases. This is consistent with recent theoretical predictions. Small angle neutron scattering measurements of these samples show both small angle scattering and quasi-Bragg peaks. As the molar ratio of ionic to nonionic surfactant increases, the low-q scattering intensity decreases and higher order quasi-Bragg peaks appear. These changes in the bulk neutron scattering signal are consistent with the changes observed with reflectivity.

1. Introduction

Small amounts of ionic surfactants have a significant influence on the behavior of dilute solutions of nonionic surfactant bilayers.[1−3] Dilute lamellar (L_α) phases of nonionic surfactants are thought[4] to be stabilized by the Helfrich undulation repulsion.[5] Adding small amounts of ionic surfactants suppresses the Helfrich undulations, flattens the bilayers, and decreases interbilayer spacing.[3] Measurements of charged L_α phases[6−10] show that unscreened electrostatic interactions allow only small undulations and that screening the electrostatic interactions with added monovalent electrolyte increases them. The effect of electrostatic interactions on undulations in charged L_α phases has been the subject of a number of theoretical investigations,[11−18] but as yet there are few quantitative comparisons between theory and experiment.[18] As noted by Li et al.,[19] neutron reflectometry[20] offers a direct way of probing undulations of surfactant bilayers close to an interface. Li et al. investigated the structure of bis(2-ethylhexyl) sulfosuccinate (AOT)−water mixtures at the air−liquid interface. For lamellar mixtures at concentrations well above the critical micelle concentration (0.11% for AOT) they observed a multilayer structure next to the air−liquid interface, but they did not fit these data to obtain estimates for the undulation amplitudes of the bilayers.

Here we use neutron scattering techniques to measure both bulk and interfacial properties of lamellar mixtures of pentaethylene glycol *n*-dodecyl ether ($C_{12}E_5$) and sodium decyl sulfonate ($C_{10}SO_3Na$) in D_2O. The results of the reflectivity measurements are compared with the results of the bulk small angle scattering measurements for several samples with different amounts of charged surfactants. Undulation amplitudes of the mixed surfactant bilayers close to the solid−liquid interface are estimated from model fits of the reflectivity data and compared to results of a recent theory for undulations in salt-free charged lamellar phases.[18]

2. Theory

Electrostatic interactions affect undulations in two ways. The presence of electric double layers stiffens the surfactant bilayers, thus suppressing undulations. Provided the correlation length ξ of the undulations is much longer than the screening length λ of the electrostatic interactions, this effect can be accounted for by introducing an electrostatic contribution to the bending modulus of the bilayers. This can be calculated within the context of the Poisson−Boltzmann equation.[21−23] Undulations are

† Part of the Special Issue "Clifford A. Bunton: From Reaction Mechanisms to Association Colloids; Crucial Contributions to Physical Organic Chemistry".

(1) Douglas, C. B.; Kaler, E. W. *J. Chem. Soc., Faraday Trans.* **1994**, *90*, 471.
(2) Jonströmer, M.; Strey, R. *J. Phys. Chem.* **1992**, *96*, 5993.
(3) Schomäcker, R.; Strey, R. *J. Phys. Chem.* **1994**, *98*, 3908.
(4) Bagger-Jörgensen, H.; Olsson, U. *Langmuir* **1996**, *12*, 413.
(5) Helfrich, W. *Z. Naturforsch.* **1978**, *33a*, 305.
(6) Bassereau, P.; Marignan, J.; Porte, G. *J. Phys. (Paris)* **1987**, *48*, 673.
(7) Roux, D.; Safinya, C. R. *J. Phys. (Paris)* **1988**, *49*, 307.
(8) Bassereau, P.; Appel, J.; Marignan, J. *J. Phys. II* **1992**, *2*, 1257.
(9) Nallet, F.; Roux, D.; Prost, J. *Phys. Rev. Lett.* **1989**, *62*, 276.
(10) Auguste, F.; Barois, P.; Fredon, L.; Clin, B.; Dufourc, E. J.; Bellocq, A. M. *J. Phys. II* **1994**, *4*, 2197.
(11) Evans, E. A.; Parsegian, V. A. *Proc. Natl. Acad. Sci. U.S.A.* **1986**, *83*, 7131.
(12) Pincus, P.; Joanny, J.; Andelman, D. *Europhys. Lett.* **1990**, *11*, 763.
(13) Evans, E.; Ipsen, J. *Electrochim. Acta* **1991**, *36*, 1735.
(14) Podgornik, R.; Parsegian, V. A. *Langmuir* **1992**, *8*, 557.
(15) Odijk, T. *Langmuir* **1992**, *8*, 1690.
(16) Odijk, T. *Europhys. Lett.* **1993**, *24*, 177.
(17) de Vries, R. *J. Phys. II* **1994**, *4*, 1541.
(18) de Vries, R. *Phys. Rev. E* **1997**, *56*, 1879.
(19) (a) Li, Z. X.; Lu, J. R.; Thomas, R. K.; Penfold, J. *Faraday Discuss.* **1996**, *104*, 127. (b) Li, Z. X.; Thirtle, P. N.; Weller, A.; Thomas, R. K.; Penfold, J.; Webster, J. R. P.; Rennie, A. R. *Physica B* **1998**, *248*, 171.
(20) For a review on neutron reflectivity, see: Russel, T. P. *Mater. Sci. Rep.* **1990**, *5*, 171.

10.1021/la990564k CCC: $19.00
Published on Web 11/17/1999

also suppressed by the electrostatic repulsion between neighboring bilayers. If the orientational order of the lamellar phase is high and $\xi \gg \lambda$ neighboring pieces of undulating bilayer effectively interact as flat planes.[15] Recently, a general harmonic theory was proposed for undulations in salt-free charged lamellar phases.[18] Predictions of that theory for the fractional area of bilayer stored in the undulations were found to be in semiquantitative agreement with the results of light-scattering experiments on weakly charged salt-free lamellar phases.[3] This section outlines the theory of undulations in salt-free charged lamellar phases following ref 18.

For monovalent counterions, in the absence of added electrolyte, the Poisson−Boltzmann result for the electrostatic potential $\psi(y)$ between two parallel, uniformly charged flat planes separated by a distance D and carrying σ elementary charges e per unit area is

$$\psi(y) = \frac{2k_BT}{e}\ln(\cos(y/\lambda))$$
$$y = -D/2 \ldots D/2 \tag{1}$$

where k_B is Boltzmann's constant and T is the absolute temperature. The screening length λ of the electrostatic interactions is

$$\lambda = {}^1/_2 D/\varphi \tag{2}$$

with

$$\varphi \tan \varphi = \Lambda \tag{3}$$

The relevant dimensionless surface charge density Λ is

$$\Lambda = \pi\sigma L_B D \tag{4}$$

where the Bjerrum length $L_B = e^2/\epsilon k_B T$ and ϵ is the permittivity of the aqueous solvent. Typically, the screening length λ is of the order of the distance D between the bilayers. Undulation amplitudes in salt-free charged lamellar phases are expected to be small with respect to the screening length λ of the electrostatic interactions, and hence the statistical mechanics of the undulations can be dealt with in a harmonic approximation, in which the energy of the undulations is assumed to be quadratic in the undulation amplitudes.

The harmonic long-wavelength approximation[18] for undulations in salt-free charged lamellar phases holds if furthermore $\xi \gg \lambda$. In this approximation the correlation length is[17,18]

$$\xi = (k_c/V''(D))^{1/4} \tag{5}$$

The potential of interaction $V(D)$ of two flat charged bilayers on a distance D follows from eq 1, so $V''(D)$, in units of k_BT is

$$V''(D) = \frac{4}{\pi L_B D^3} g_1(\Lambda) \tag{6}$$

$$g_1(\Lambda) = \frac{\varphi^2(\Lambda^2 + \varphi^2)}{\Lambda^2 + \Lambda + \varphi^2} \tag{7}$$

The bending modulus k_c now includes an electrostatic contribution

$$k_c = k_{c,0} + k_{c,el} \tag{8}$$

For salt-free charged lamellar phases, the electrostatic contribution to the bending modulus of in-phase undulations was recently calculated[24] from the Poisson−Boltzmann equation, with the result that, in units of k_BT

$$k_{c,el} = \frac{D}{\pi L_B} g_2(\Lambda) \tag{9}$$

$$g_2(\Lambda) = \frac{\Lambda(2\Lambda + 1 - \varphi^2)}{\Lambda^2 + \varphi^2} - (1 + \varphi^2/3) \tag{10}$$

This generalizes previous results for the limiting cases $\Lambda \ll 1$[25] and $\Lambda \gg 1$.[26]

To calculate undulation amplitudes, let $u_n(\vec{x})$ be the instantaneous undulation amplitude of the nth bilayer in the lamellar stack at $\vec{x}$, where $\vec{x}$ are the coordinates in the plane of the bilayer. As is usual for a smectic-A, the absolute mean-square undulation amplitudes $\langle u_n^2(\vec{x})\rangle$ diverge logarithmically with system size. On the other hand, the relative mean-square undulation amplitudes

$$d^2 \equiv \langle (u_{n+1}(\vec{x}) - u_n(\vec{x}))^2 \rangle \tag{11}$$

are finite and are related to the typical undulation wavelength ξ by[17]

$$d^2 = \xi^2/2\pi k_c \tag{12}$$

where k_c is again in units of k_BT. Thus the undulation amplitude in the harmonic long-wavelength approximation is

$$d^2 = {}^1/_2 L_B D(g_1(\Lambda)(g_2(\Lambda) + \pi L_B k_{c,0}/D))^{-1/2} \tag{13}$$

Unfortunately, for typical charge densities and intrinsic bending moduli, correlation lengths calculated according to eq 5 are of the order of the screening length of the electrostatic interactions, rather than much longer. Hence the long-wavelength approximation is only marginally valid. The recent more general harmonic theory[18] is also valid if the correlation length ξ of the undulations is of the order of, or less than, the screening length λ. The general harmonic theory accounts for the disappearance of the electrostatic stiffening effect at wavelengths much smaller than the screening length. It also accounts for the vanishingly small electrostatic compressional energy of short wavelength undulations. Both effects increase the undulation amplitudes above the predictions of the long-wavelength approximation. Within the general harmonic theory, the expression for the undulation amplitude valid for all ξ and λ is

$$d^2 = {}^1/_2 L_B D \int_0^\infty x\, dx \frac{1}{f_o(x,\Lambda) - f_e(x,\Lambda)} \times \left(1 - \left(\frac{f_e(x,\Lambda)/x^4 + \pi L_B k_{c,0}/D}{f_o(x,\Lambda)/x^4 + \pi L_B k_{c,0}/D}\right)^{1/2}\right) \tag{14}$$

(21) Winterhalter, M.; Helfrich, W. *J. Phys. Chem.* **1988**, *92*, 6865.
(22) Mitchell, D. J.; Ninham, B. W. *Langmuir* **1989**, *5*, 1121.
(23) (a) Lekkerkerker, H. N. W. *Physica A* **1990**, *159*, 319. (b) Lekkerkerker, H. N. W. *Physica A* **1990**, *167*, 384.
(24) Fogden, A.; Daicic, J.; Mitchell, D. J.; Ninham, B. W. *Physica A* **1996**, *234*, 167.
(25) Harden, J. L.; Marques, C.; Joanny, J.-F.; Andelman, D. *Langmuir* **1992**, *8*, 1170.
(26) Higgs, P. G.; Joanny, J.-F. *J. Phys. (Paris)* **1990**, *51*, 2307.

with

$$f_e(x,\Lambda) = \frac{(\Lambda^2 + \varphi^2)x(\varphi^2 \sinh x - \Lambda x \cosh x)}{(\Lambda^2 + \varphi^2 + x^2)\cosh x - \Lambda x \sinh x} + x^2(\Lambda - \varphi^2) \quad (15)$$

$f_o(x,\Lambda)$ is obtained by switching sinh and cosh in eq 15. Expanding the functions $f_{e,o}(x,\Lambda)$ in eq 14 up to fourth order in x around $x = 0$ yields the harmonic long-wavelength result, eq 13. Typically the undulation amplitudes d of the harmonic long-wavelength approximation eq 13 match those of the full theory (eq 14) to within about 20%.

3. Materials and Methods

Materials and Sample Preparation. D_2O was purchased from Cambridge Isotope Laboratory (deuteration 99.9%, low paramagnetic, low conductivity). Pentaoxyethylene glycol dodecyl monoether ($C_{12}E_5$) was purchased from Nikko Surfactants (99+% purity) and was used as received. Anionic surfactant sodium decylsulfonate ($C_{10}SO_3Na$) was purchased from Lancaster Synthesis (98%) and was used as received. Octadecyltrichlorosilane ($Cl_3Si-(CH_2)_{17}-CH_3$) was purchased from Aldrich, with quoted purity >95%. A finely polished silicon block (type N, 111 orientation) was purchased from Semiconductor Processing Co. in Boston, MA.

Samples were made by weight, with the dilute samples made by dilution of stock solutions. Stock solutions were deoxygenated with argon before use. The phase behavior of $C_{12}E_5-C_{10}SO_3Na-D_2O$ mixture was observed in a water bath with stability of ± 0.1 °C at a fixed weight fraction of $C_{12}E_5$ in D_2O and as a function of molar ratio (R) of anionic to nonionic surfactant.

Small Angle Neutron Scattering. Small angle neutron scattering experiments were performed using the NG7 30-m spectrometer at the National Institute of Standards and Technology (NIST) in Gaithersburg, MD. The range of the scattering vector, $q = (4\pi/\lambda)\sin(\theta/2)$, was $0.0047 < q/\text{Å}^{-1} < 0.6$. The wavelength was $\lambda = 6$ Å, with wavelength spread of $\Delta\lambda/\lambda = 10\%$. The samples were measured in 1 mm Hellma QS cells at the operating temperature of 57 °C, with a stability of ±0.1 °C. The efficiency of the detector was determined using the incoherent scattering of water, and experimental data were corrected for empty cell and background scattering and normalized to an absolute scale using the supplied calibration standards.

Neutron Reflectivity. The sample compartment consists of three main parts, namely, a finely polished silicon wafer (4 in. diameter, 1 in. thick), a custom designed quartz disk, and a noncorrosive, high-temperature resistant O-ring (~3.5 in. i.d.). The assembly is shown in Figure 1. Silicon was used as a substrate because it absorbs neutrons weakly. The sample temperature in the cell was set to 57 °C and was controlled by water circulation. A thermocouple was placed in the hollow tube inside the quartz cell to measure the temperature close to the sample. The sample was equilibrated at 57 °C and was injected into the cell through a 30-cm^3 custom-made water-jacketed syringe. To induce strong surface ordering of the lamellae, the silicon surface was treated with octadecyltrichlorosilane ($Cl_3Si-(CH_2)_{17}-CH_3$, OTS) to form a hydrophobic monolayer of $O_3Si-(CH_2)_{17}-CH_3$.[27] The thickness of the alkyl tails was 17 Å (as measured by X-ray reflectivity) and is similar to thicknesses reported in the literature.[28]

The NG7 neutron reflectometer at NIST was used with monochromated neutrons ($\lambda = 4.77$ Å, $\Delta\lambda = 0.18$ Å), counted with a He^3 gas-filled detector. The background (off-specular) due to small angle scattering from the bulk was measured as a function of q by rotating the sample away from the specular condition. Data were collected over a q_z range from 0 to 0.12 Å^{-1}, where q_z is the normal component of the incident neutron momentum in a vacuum.

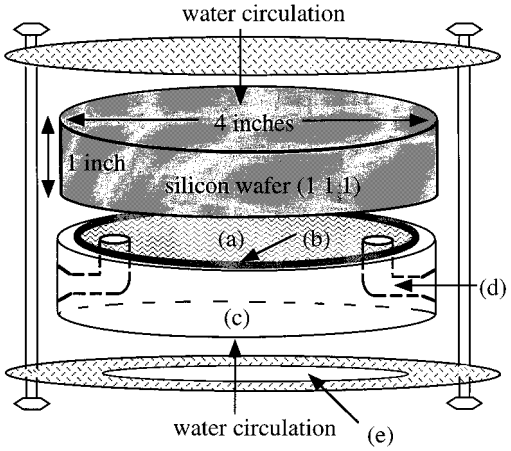

Figure 1. Schematic of the sample compartment for neutron reflectivity measurements: a, sample; b, O-ring; c, quartz block; d, sample port; e, Plexiglas window. Sample is injected through a 30-cm^3 water-jacketed glass syringe at 57 °C. After injection, the ports are closed by stopcocks. The Plexiglas window allows for sample inspection.

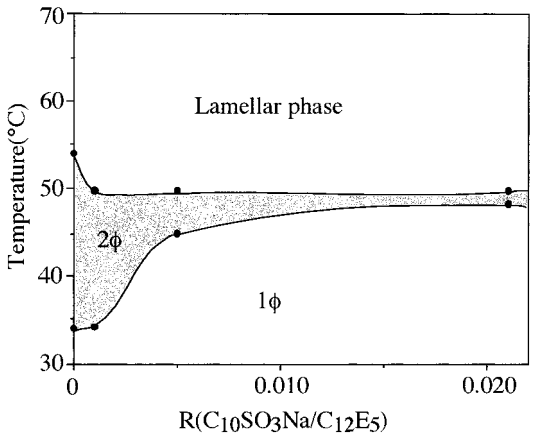

Figure 2. Phase map of $C_{12}E_5-C_{10}SO_3Na-D_2O$ mixtures as a function of molar ratio (R) of charged surfactant to nonionic surfactant. The weight fraction of $C_{12}E_5$ is fixed at 0.08 in D_2O. The 1ϕ phase is isotropic, and the two-phase region is shaded.

4. Results

The lamellar mixtures studied here all have a fixed weight fraction of 0.08 of $C_{12}E_5$ in D_2O, corresponding to a bilayer volume fraction ϕ_s of 0.095. The amount of ionic surfactant is specified by the molar ratio R of ionic to nonionic surfactant. Figure 2 shows the phase behavior of the $C_{12}E_5-C_{10}SO_3Na-D_2O$ mixtures at $\phi_s = 0.095$, as a function of R and temperature. Adding charged surfactants to the nonionic mixture causes the L_α phase to form at lower temperature and to remain stable at higher temperatures.

Small angle neutron scattering spectra were measured at 57 °C, for $C_{12}E_5-C_{10}SO_3Na-D_2O$ lamellar mixtures at $R = 0.001$, 0.005, and 0.021. The spectra (Figure 3) show Caillé[29] quasi-Bragg peaks typical of smectic A liquid crystals. The number of quasi-Bragg peaks as well as the intensity of the peaks increases with added $C_{10}SO_3Na$ and, simultaneously, the low-q scattering drops substantially. These observations indicate increased orientational order of the lamellae and smaller undulation amplitudes as the amount of ionic surfactant increases. Table 1 shows the

(27) Salamat, G. Thesis, University of Delaware, 1998.
(28) Tidswell, I. M.; Ocko, B. M.; Pershan, P. S.; Wasserman, S. R.; Whitesides, G. M.; Axe, J. D. *Phys. Rev., B* **1990**, *41*, 1111.
(29) Caillé, A. *C. R. Seances Acad. Soc., Ser. B* **1972**, *274*, 891.
(30) Helfrich, W. *Z. Naturforsch.* **1975**, *30c*, 841.
(31) Strey, R.; Glatter, O.; Schubert, K.-V.; Kaler, E. W. *J. Chem. Phys.* **1996**, *105*, 1175.

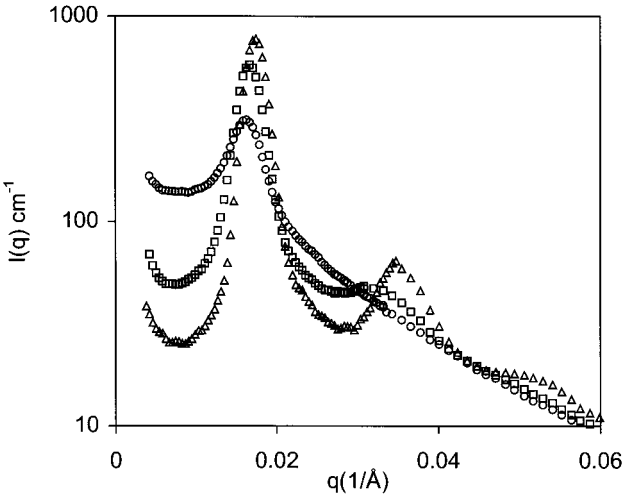

Figure 3. Small angle neutron scattering spectra $I(q)$ as a function of q for $C_{12}E_5-C_{10}SO_3Na-D_2O$ lamellar mixtures at 57 °C, for $R = 0.001$(○), $R = 0.005$ (□), and $R = 0.021$ (△). R is the molar ratio of ionic to nonionic surfactant.

Table 1. The Lamellar Repeat Distance $\tilde{D} = 2\pi/q_{max}$ As Determined from the Position q_{max} of the First-Order Bragg Peak and the Apparent Bilayer Thickness $\delta_{app} = \phi_s\tilde{D}$ for $C_{12}E_5-C_{10}SO_3Na-D_2O$ Lamellar Mixtures[a]

R	$\tilde{D} = 2\pi/q_{max}$ (Å)	$\delta_{app} = \phi_s\tilde{D}$ (Å)
0.001	385	36.5
0.005	376	35.7
0.021	359	34

[a] R is the molar ratio of charged surfactant to nonionic surfactant. The total bilayer volume fraction ϕ_s is equal to 0.095.

lamellar repeat distances $\tilde{D} = 2\pi/q_{max}$, obtained from the position q_{max} of the first-order peaks. The repeat distance $\tilde{D}$ is related to the bilayer volume fraction ϕ_s and bilayer thickness δ via

$$\phi_s\tilde{D} \equiv \delta_{app} = \delta\left(1 + \frac{\Delta A}{A}\right) \qquad (16)$$

where $\Delta A/A$ is the fractional area of bilayer stored in thermal undulations.[30] Increased undulation amplitudes will thus be reflected in an increased apparent bilayer thickness δ_{app}. Indeed, as shown in Table 1, the apparent bilayer thickness is largest for the sample with the lowest amount of ionic surfactant ($R = 0.001$), for which undulations are expected to be most pronounced. Furthermore, the apparent thicknesses are appreciably larger than the intrinsic thickness of the $C_{12}E_5$ bilayers, which is $\delta \approx 30$ Å,[32] indicating that an appreciable amount of bilayer area is stored in the undulations, even for the more highly charged samples.

The background-subtracted neutron reflectivity at 57 °C of samples with $R = 0.001$, $R = 0.005$, and $R = 0.021$, as a function of the perpendicular wavevector q, is shown in Figure 4. All spectra show Bragg peaks, indicating a multilayer structure next to the silicon wall. The number of Bragg peaks and their intensity increase as the amount of ionic surfactants is increased. This again indicates increased orientational order of the lamellae and smaller undulation amplitudes in samples with larger amounts of ionic surfactant.

Also shown in Figure 4 are model fits to the reflectivity data based on a model for the scattering length density profile $\rho(z)$ as a function of the distance z to the silicon wall. The model profiles $\rho(z)$ are shown in Figure 5. They consist of two main parts corresponding to the composite film next to the silicon block and to the dispersed bilayers in D_2O. The film next to the silicon block contains a series of layers in the following order: SiO_2, an intermediate layer,[28] the chemisorbed alkyl chains, the alkyl chains of $C_{12}E_5$ (the contribution of $C_{10}SO_3Na$ to the value of the scattering length density was insignificant), and the ethoxy headgroup of $C_{12}E_5$ plus 10 molecules of D_2O that hydrate each surfactant headgroup.[31] The scattering

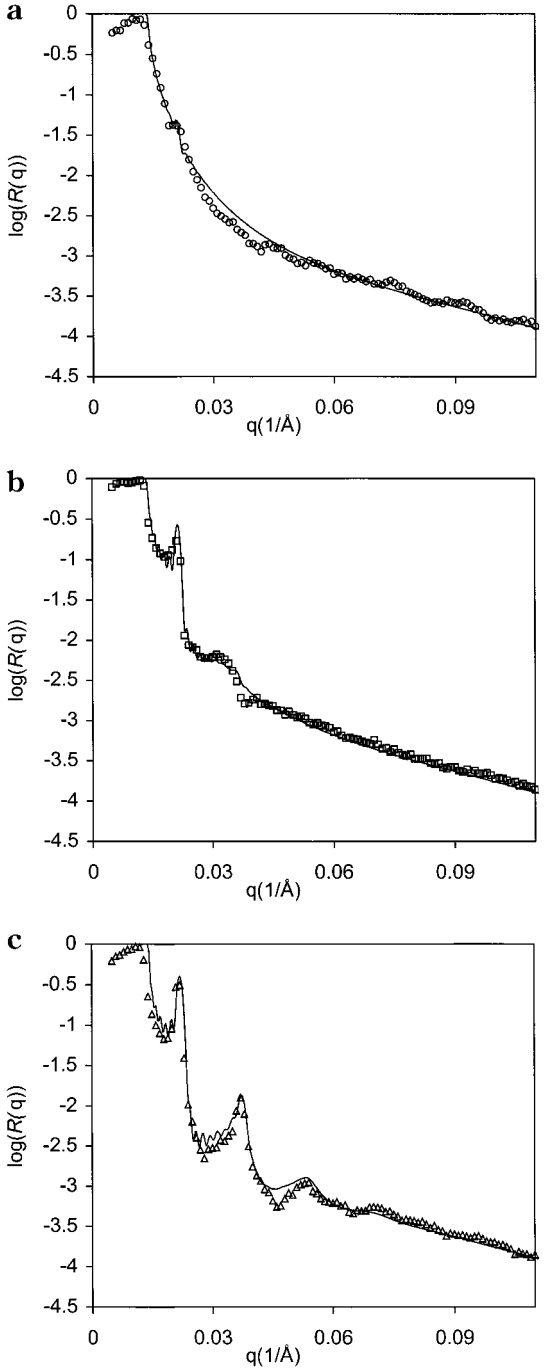

Figure 4. Neutron reflectivity $R(q)$ as a function of q for $C_{12}E_5-C_{10}SO_3Na-D_2O$ lamellar mixtures at the silicon−lamellar interface at 57 °C, for (a) $R = 0.001$, (b) $R = 0.005$, and (c) $R = 0.021$. R is the molar ratio of charged surfactant to nonionic surfactant. Solid curves are theoretical reflectivity curves based on the model scattering length densities $\rho(z)$ shown in Figure 5. Theoretical reflectivity curves are convoluted for the instrument resolutions ($\Delta\theta = 2 \times 10^{-4}$, $\Delta\lambda = 0.18$ Å) using a Gaussian resolution function.

(32) Strey, R.; Schomäcker, R.; Roux, D.; Nallet, F.; Ollson, U. *J. Chem. Soc., Faraday Trans.* **1990**, *86*, 2253.

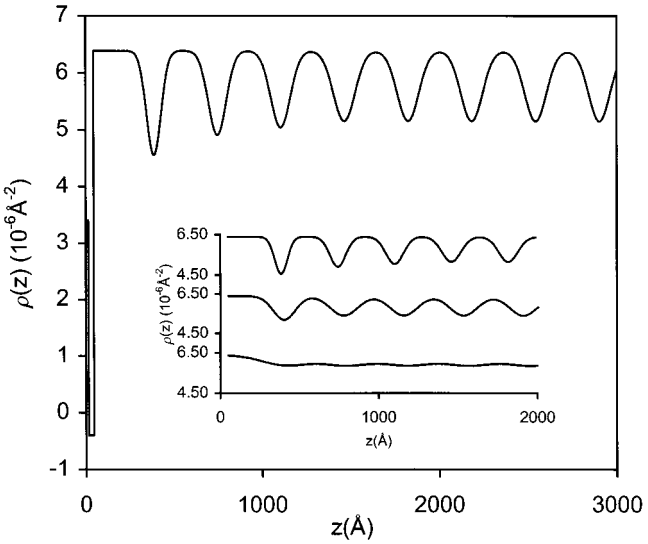

Figure 5. Model scattering length density $\rho(z)$ as a function of the distance z away from the silicon block used for the fit of Figure 4c, for $R = 0.021$. Inset shows a comparison of the model scattering length densities for 100 Å $\leq z \leq$ 2000 Å used for the fits of Figure 4a (bottom curve), Figure 4b (middle curve) and Figure 4c (top curve) for respectively $R = 0.001$, $R = 0.005$, and $R = 0.021$.

length density of this composite film is modeled by an initial layer of scattering length density $\rho_{SiO_2} = 3.4 \times 10^{-6}$ Å^{-2} and thickness z_{SiO_2} representing the silicon oxide layer, followed by a layer of low scattering length density $\rho_{Alkyl} = -4 \times 10^{-7}$ Å^{-2} and thickness z_{Alkyl} representing the chemisorbed alkyl chains and the absorbed monolayer of $C_{12}E_5$ and $C_{10}SO_3Na$. Including interfacial roughness in this part of the profile, or including a separate layer representing the EO_5 headgroups of the nonionic surfactants, does not significantly improve the quality of the fits. The surfactant bilayers themselves are modeled as having a uniform scattering length density $\rho_{bilayer} = 1.26 \times 10^{-7}$ Å^{-2} and a thickness $\delta = 30$ Å.[32] The average position z_n away from the silicon block of the center of the nth bilayer is such that the distance between succesive bilayers (and between the film next to the silicon block and the first bilayer) is $D = \tilde{D} - \delta$, with $\tilde{D}$ taken from Table 1. Fluctuations of the position z of the nth bilayer away from its average position z_n are assumed to have a Gaussian distribution $p_n(z)$

$$p_n(z) = \frac{1}{\sqrt{2\pi u_n}} \exp\left(-\frac{1}{2}(z - z_n)^2/u_n^2\right) \qquad (17)$$

where u_n is the root-mean-square amplitude of the undulations of the nth bilayer. The scattering length density $\rho(z)$ thus obtained for the bilayers dispersed in D_2O is

$$\rho(z) = \rho_{D_2O} + (\rho_{bilayer} - \rho_{D_2O}) \sum_{n=1}^{N} \int_{z-\delta/2}^{z+\delta/2} dz'\, p_n(z') \qquad (18)$$

The scattering length density ρ_{D_2O} of D_2O is $\rho_{D_2O} = 6.39 \times 10^{-6}$ Å^{-2}. Integrating over z' gives

$$\rho(z) = \rho_{D_2O} + \frac{1}{2}(\rho_{bilayer} - \rho_{D_2O}) \sum_{n=1}^{N} \left\{ \mathrm{erf}\left(\frac{||z - z_n| + {}^1/_2\delta|}{\sqrt{2u_n}}\right) + \mathrm{sgn}({}^1/_2\delta - |z - z_n|)\, \mathrm{erf}\left(\frac{||z - z_n| - {}^1/_2\delta|}{\sqrt{2u_n}}\right) \right\} \qquad (19)$$

where

$$\mathrm{sgn}(x) = \begin{cases} -1 & x < 0 \\ 0 & x = 0 \\ 1 & x > 0 \end{cases} \qquad (20)$$

Reflectivity curves are calculated from the model scattering length density profiles by discretizing the profile into sufficiently many layers of constant scattering length density, and applying the Parrat[33] recursion formula using a recently developed spreadsheet-based computer program.[34] The model reflectivity curves are convoluted for experimental resolutions ($\Delta\theta = 2 \times 10^{-4}$, $\Delta\lambda = 0.18$ Å) using a Gaussian resolution function. The total number of dispersed bilayers N taken into account in the model profiles was set to $N = 8$. Increasing N beyond this value does not significantly improve the quality of the fits.[35] The parameters z_{Alkyl} and z_{SiO_2} were set to 30 and 15 Å, respectively, for the fits in Figure 4. The fitted values of the undulation amplitudes u_n are collected in Table 2. For $R = 0.001$, no significant improvement was obtained in the quality of the fits by allowing for a variation of the undulation amplitudes u_n as a function of n. Furthermore, since for this sample the Bragg peak is very weak (Figure 4a), the fitted value of the undulation amplitude is only a rough estimate. For $R = 0.005$, an improved quality of fit was obtained by allowing a difference between the undulation amplitude for $n = 1$ and those for $n > 1$. Finally, for $R = 0.021$ it was essential to include a variation of u_n up to $n = 4$ to obtain a reasonable fit, although the values of the fitted undulation amplitudes for $n > 1$ are again estimates, since the neutron reflectivity is mostly sensitive to the undulation amplitude of the first bilayer.

Although the model scattering length density profiles are highly idealized in the sense that they assume perfect lamellar ordering parallel to the silicon block, they nevertheless capture the essential features of the observed reflectivity. Also, the model fits demonstrate clearly the expected trend of decreasing undulation amplitudes as the concentration of ionic surfactant is increased.

5. Discussion

For thin smectic films both theory and experiment confirm that undulations are suppressed at the interfaces and are largest in the center of the film.[36] Similarly, for smectic phases next to a solid wall, undulations close to the wall are expected to be suppressed with respect to those in the bulk. Away from the wall undulation amplitudes are expected to increase and, ultimately, in the bulk of the smectic phase, to diverge logarithmically with system size due to the smectic long-wavelength

(33) Parratt, L. G. *Phys. Rev.* **1954**, *95*, 359.
(34) Welp, K. A.; Co, C. C.; Wool, R. P. *J. Neutron Res.*, in press.
(35) The small oscillations in the fit for $R = 0.021$ only disappear at very much larger values of N. Such values of N can no longer be handled by the fit program at the desired level of resolution in the z-direction.
(36) (a) Hoylst, R.; Tweet, D. J.; Sorensen, L. B. *Phys. Rev. Lett.* **1990**, *65*, 2153. (b) Tweet, D. J.; Hoylst, R.; Swanson, B. D.; Stragier, H.; Sorensen, L. B. *Phys. Rev. Lett.* **1990**, *65*, 2157.

Table 2. Undulation Amplitudes u_n of the nth Bilayer Away from the Silicon Block As Determined from Model Fits of Neutron Reflectivity of $C_{12}E_5$−$C_{10}SO_3Na$−D_2O Lamellar Mixtures[a]

R	u_1 (Å)	u_2 (Å)	u_3 (Å)	u_4 (Å)
0.001	150			
0.005	70	85		
0.021	40	50	55	60

[a] R is the molar ratio of ionic surfactant to nonionic surfactant. For $R = 0.001$, $u_n = u_1$ for $n > 1$, for $R = 0.005$, $u_n = u_2$ for $n > 2$, and for $R = 0.021$, $u_n = u_4$ for $n > 4$.

Table 3. Comparison of Theoretical Predictions of the Bulk Relative Undulation Amplitudes in the Long-Wavelength Approximation (d_{long}), and in the General Harmonic Approximation (d_{gen}), with Absolute Undulation Amplitudes u_1 of Bilayers Next to a Silicon Wall, As Determined Experimentally by Fitting Neutron Reflectivity Data for $C_{12}E_5$−$C_{10}SO_3Na$−D_2O Lamellar Mixtures[a]

R	Λ	$k_{c,el}(k_BT)$	d_{long} (Å)	d_{gen} (Å)	u_1 (Å)
0.001	0.14	0.04	86	103	150
0.005	0.69	0.55	54	64	70
0.021	2.70	1.96	35	40	40

[a] R is the molar ratio of ionic surfactant to nonionic surfactant. Also indicated are the dimensionless surface charge density Λ of the bilayers and the Poisson−Boltzmann prediction for the electrostatic contribution $k_{c,el}$ to the bending modulus.

fluctuations. Consistent with these expectations, the fitted values of the undulation amplitudes measured here indicate increased undulation amplitudes for bilayers further away from the silicon block.

The theoretical and fitted values of undulation amplitudes are compared in Table 3. In view of the limited sensitivity of neutron reflectivity to undulation amplitudes of bilayers further away from the silicon block, only the fitted value u_1 of the undulation amplitude of the first bilayer is included in the comparison. They are compared to both the prediction d_{long} of the harmonic long-wavelength approximation (eq 12) and the prediction d_{gen} of the general harmonic theory (eq 14). Table 3 also gives the values of the dimensionless surface charge density Λ[38] and the Poisson−Boltzmann predictions for the electrostatic contribution $k_{c,el}$ to the bending modulus of the bilayers. In calculation of the undulation amplitudes, a typical value[18,32] of $k_{c,0} = 2k_BT$ was assumed for the intrinsic bending modulus of the $C_{12}E_5$ bilayers. The theoretical predictions for the relative bulk undulation amplitudes are of the same order of magnitude as the fitted values u_1 of the undulation amplitudes of the bilayers next to the silicon block, for all three values of the molar mixing ratio R, as expected.[37] Except for the most weakly charged sample, the undulation amplitudes are appreciably smaller than the interbilayer distance D (Table 1); hence these lamellar phases are indeed stabilized by unscreened electrostatic repulsion rather than by the Helfrich undulation repulsion. The theoretical predictions for the relative bulk undulation amplitudes suggest that the $R = 0.001$ lamellar phases are still electrostatically stabilized, but since the fitted undulation amplitude u_1 is only an estimate, the presence of steric repulsion for the $R = 0.001$ lamellar phases cannot be ruled out.

The h-AOT salt-free charged lamellar phases studied by Li et al.[19] show reflectivity curves having three distinct Bragg peaks and are very similar to the $R = 0.021$ curve of Figure 4c. Li et al. report that these lamellar phases are stabilized by Helfrich undulations. However, in the light of the present quantitative analysis it is more likely that the salt-free AOT lamellar phase is also stabilized by unscreened electrostatic repulsion and has undulation amplitudes appreciably smaller than the interbilayer distance. Li et al. also measured the off-specular reflectivity of the h-AOT lamellar phase at the air−liquid interface, finding qualitative evidence for correlations between the undulations of different bilayers. Unfortunately, analysis of this off-specular scattering within the present framework would be cumbersome and would likely require the distorted-wave Born approximation.[39]

6. Conclusion

Neutron reflectometry offers a unique and direct way to estimate undulation amplitudes of surfactant bilayers close to the solid−liquid interface. For $C_{12}E_5$−$C_{10}SO_3Na$−D_2O lamellar phases it is found that they are stabilized by unscreened electrostatic repulsion rather than by Helfrich undulation repulsion and have undulation amplitudes that are consistent with theoretical predictions.

Note Added in Proof

Estimates of the relative bulk undulation amplitudes d_{und} have been obtained by fitting the small angle neutron scattering spectra of Figure 3 using the model of Nallet et al.[40] We find, for $R = 0.001$, $d_{und} = 90$ Å, for $R = 0.005$, $d_{und} = 60$ Å, and for $R = 0.021$, $d_{und} = 40$ Å, in good agreement with both the theoretical predictions and the values obtained from neutron reflectivity (see Table 3).

Acknowledgment. We are grateful for the financial support of the National Science Foundation (CTS 9814399) and acknowledge the support of the National Institute of Standards and Technology, U.S. Department of Commerce, for providing the neutron research facilities used in this work. This work is also supported by The Netherlands Organization for Scientific Research (NWO). We are grateful to Pat Gallagher and Richard Zielinski for their technical assistance. R.d.V. thanks K. Welp and C. Co for useful discussions on neutron reflectivity and for help with fitting the neutron reflectivity data.

LA990564K

(37) Both the undulation amplitude of the bilayers next to the wall and the relative undulation amplitude in the bulk of the lamellar phase are set by the typical wavelength or correlation length ξ of the undulations, and scale according to eq 12, though with possibly different numerical prefactors.

(38) We assume that all the ionic surfactants are dissociated and incorporated into the bilayers.[3] Hence the surface charge density is taken to be $\sigma = R/a$, where R is the mixing ratio of ionic to nonionic surfactant, and $a \approx 0.6$ nm^2 is the headgroup area of the $C_{12}E_5$ molecules.[3]

(39) See e.g.: (a) Sinha, S. K.; Sirota, E. B.; Garoff, S.; Stanley, H. B. *Phys. Rev. B* **1988**, *38*, 2297. (b) Pynn, R. *Phys. Rev. B* **1992**, *45*, 602. (c) Daillant, J.; Quinn, K.; Gourier, C.; Rieutord, F. *J. Chem. Soc., Faraday Trans.* **1996**, *92*, 505.

(40) Nallet, F.; Laversanne, R.; Roux, D. *J. Phys. II* **1993**, *3*, 487.